cipitation assays (12). Thus, in keeping with the late inhibition of DNA binding by NF-κB (Fig. 1), newly synthesized IκBα can physically associate with p65. Furthermore, immunofluorescent staining of COS-7 cells transfected with the p65 expression vector confirmed that the newly synthesized IκBα was primarily localized in the cytoplasm (Fig. 4C), a finding that is fully consistent with the known subcellular location of inactive NF-κB complexes in resting human T cells (4, 11).

Because IκBα rapidly disappears after its release from NF-κB (Fig. 1), another potential mechanism of IκBα regulation could involve the stabilization of this labile molecule when complexed with p65 in the cytoplasm (7). To compare the relative half-life ($T_{1/2}$) of survival of free and p65-complexed IκBα, pulse-chase experiments (Fig. 5) were performed in COS-7 cells transfected with an IκBα expression vector in the absence or presence of vectors encoding p65 deletion mutants differing in their capacity to complex with IκBα. These COOH-terminal deletion mutants lacking a transactivation domain were selected to preclude the induction of endogenous IκBα expression. Mutant p65(1–312) possesses a fully functional IκBα binding domain whereas mutant p65(1–270) fails to bind IκBα (15). In the absence of either of these truncated p65 proteins, IκBα was rapidly degraded ($T_{1/2} \approx 40$ min). In contrast, in the presence of p65(1–312), the intracellular half-life of IκBα was extended to more than 4 hours. However, with p65(1–270), IκBα exhibited a $T_{1/2}$ indistinguishable from that observed in cells transfected with IκBα alone. These findings suggest that the intracellular survival of IκBα is prolonged when this cytoplasmic inhibitor associates with p65.

In summary, these findings indicate that IκBα is a physiological inhibitor of the heterodimeric NF-κB complex whose expression is induced by NF-κB in activated T cells. Specifically, this particular inhibitor is rapidly degraded in PMA- or TNF-α–stimulated human T cells in concert with the liberation and nuclear import of NF-κB. After degradation of released IκBα, the cytoplasmic reservoir of this · inhibitor is completely replenished by NF-κB– induced de novo synthesis of IκBα protein, which is preceded by a marked increase in IκBα mRNA expression. Because IκBα mRNA induction occurs in the presence of translation inhibitors and requires functional coexpression of the transactivation and DNA binding domains of p65, it seems likely that p65 mediates the activation of IκBα gene expression by a direct mechanism. This novel autoregulatory loop provides a dynamic mechanism of feedback control for transcriptional induction mediated by NF-

κB p65, thus ensuring its rapid but transient pattern of biological action.

## REFERENCES AND NOTES

1. M. J. Lenardo and D. Baltimore, Cell 58, 227 (1989); P. A. Baeuerle and D. Baltimore, in Molecular Aspects of Cellular Regulation, Hormonal Control Regulation of Gene Transcription, P. Cohen and J. G. Foulkes, Eds. (Elsevier/North-Holland, Amsterdam, 1990), p. 409.
2. G. Nabel and D. Baltimore, Nature 326, 711 (1987).
3. J. D. Kaufman et al., Mol. Cell. Biol. 7, 3759 (1987); M. A. Muesing, D. H. Smith, D. J. Capon, Cell 48, 691 (1987); M. Siekevitz et al., Science 238, 1575 (1987); S. E. Tong-Starksen, P. A. Luciw, B. M. Peterlin, Proc. Natl. Acad. Sci. U.S.A. 84, 6845 (1987).
4. P. A. Baeuerle and D. Baltimore, Science 242, 540 (1988); Cell 53, 211 (1988).
5. M. B. Urban and P. A. Baeuerle, Genes Dev. 4, 1975 (1990); P. A. Baeuerle, Biochim. Biophys. Acta 1072, 63 (1991).
6. R. Sen and D. Baltimore, Cell 47, 921 (1986).
7. P. A. Baeuerle, M. Lenardo, J. W. Pierce, D. Baltimore, Cold Spring Harbor Symp. Quant. Biol. 53, 789 (1988).
8. E. Bohnlein et al., Cell 53, 827 (1988).
9. A. Israel et al., EMBO J. 8, 3793 (1989); J. W. Lowenthal, D. W. Ballard, E. Böhnlein, W. C. Greene, Proc. Natl. Acad. Sci. U.S.A. 86, 2331 (1989); L. Osborn, S. Kunkel, G. J. Nabel, ibid., p. 2336; N. Arima, W. A. Kuziel, T. A. Grdina, W. C. Greene, J. Immunol. 149, 83 (1992).
10. P. A. Baeuerle and D. Baltimore, Genes Dev. 3, 1689 (1989); F. Shirakawa and B. M. Mizel, Mol. Cell. Biol. 9, 2424 (1989), S. Ghosh and D. Baltimore, Nature 344, 678 (1990).
11. J. A. Molitor, W. H. Walker, S. Doerre, D. W.
12. S.-C. Sun et al., unpublished data.
13. S. Haskill et al., Cell 65, 1281 (1991).
14. H. Ohno, G. Takimoto, T. W. McKeithan, ibid. 60, 991 (1990); N. Davis et al., Science 253, 1268 (1991); J.-I. Inoue, L. D. Kerr, A. Kakizuka, I. M. Verma, Cell 68, 1109 (1992); F. G. Wulczyn, M. Naumann, C. Scheidereit, Nature 358, 597 (1992).
15. P. A. Ganchi, S.-C. Sun, W. C. Greene, D. W. Ballard, Mol. Biol. Cell 3, 1339 (1992).
16. A. A. Beg et al., Genes Dev. 6, 1899 (1992).
17. R. Schreck, P. Rieber, P. A. Baeuerle, EMBO J. 10, 2247 (1991); M. Meyer et al., ibid. 11, 2991 (1992).
18. S. Ghosh et al., Cell 62, 1019 (1990); T. D. Gilmore, ibid., p. 841; M. Kieran et al., ibid., p. 1007.
19. G. P. Nolan, S. Ghosh, H.-C. Liou, P. Tempst, D. Baltimore, ibid. 64, 961 (1991).
20. S. M. Ruben et al., Science 251, 1490 (1991).
21. D. W. Ballard et al., Proc. Natl. Acad. Sci. U.S.A. 89, 1875 (1992).
22. M. L. Schmitz and P. Baeuerle, EMBO J. 10, 3805 (1991).
23. J.-I. Inoue et al., Proc. Natl. Acad. Sci. U.S.A. 88, 3715 (1991).
24. E. Schreiber, P. Matthias, M. M. Muller, W. Schaffner, Nucleic Acids Res. 17, 6419 (1989).
25. N. M. Gough, Anal. Biochem. 173, 93 (1988).
26. A. Thornell, B. Hallberg, T. Grundstrom, Mol. Cell. Biol. 8, 1625 (1988).
27. D. W. Ballard et al., New Biol. 1, 83 (1989).
28. M. Gilman et al., Eds., Current Protocols in Molecular Biology, (Wiley, New York, 1987).
29. We thank P. Morrow and K. Koerber for technical assistance, A. Baldwin for the IκBα cDNA, S. Ruben and C. Rosen for the p65 cDNA, and our laboratory colleagues for helpful discussion. This work was supported by NIH training grant 5T32CA09111 to P.A.G.

# Activity-Dependent Regulation of Conductances in Model Neurons

Gwendal LeMasson, Eve Marder, L. F. Abbott*

Neurons maintain their electrical activity patterns despite channel turnover, cell growth, and variable extracellular conditions. A model is presented in which maximal conductances of ionic currents depend on the intracellular concentration of calcium ions and so, indirectly, on activity. Model neurons with activity-dependent maximal conductances modify their conductances to maintain a given behavior when perturbed. Moreover, neurons that are described by identical sets of equations can develop different properties in response to different patterns of presynaptic activity.

Most neurons survive for almost as long as the animal in which they are found and can retain stable electrical properties for much of the animal's lifetime. This stability results from a dynamic equilibrium because the ion channels that control the electrical activity of each neuron are replaced by protein turnover and because the neuron may change size or shape. Realistic models of neurons, with multiple active currents, are sensitive to small changes in parameters (1, 2). How then do neurons maintain stable electrical activity?

We suggest a model in which the intrinsic properties of a neuron are regulated by its activity. This model uses the intracellular $Ca^{2+}$ concentration as an indicator of activity, although other intracellular correlates of electrical activity might be involved. In the model, the maximal conductance of each ionic current is a dynamical variable rather than a fixed parameter.

We modified the model of Buchholtz and co-workers (3) that was derived from voltage-clamp data from the lateral pyloric

G. LeMasson and E. Marder, Department of Biology and Center for Complex Systems, Brandeis University, Waltham, MA 02254.
L. F. Abbott, Department of Physics and Center for Complex Systems, Brandeis University, Waltham, MA 02254.

*To whom correspondence should be addressed.

**Fig. 1.** (**A**) The pattern of activity and (**B**) time-averaged intracellular Ca²⁺ concentration for a model neuron as a function of the $\bar{g}$ of $I_{Ca}$ and $I_{KCa}$ (*14*). (**C**) Superimposition of the area in which the Ca²⁺ concentration is 0.1 to 0.3 μM, on the region where bursting is seen.



**Fig. 2.** Response of a model neuron to changes in extracellular K⁺ concentration. (**A**) Electrical activity. In (**B**) (control) and (**C**) (high extracellular K⁺), bursting is indicated by shaded regions, with a Ca²⁺ concentration between 0.1 and 0.3 μM inside the solid lines.
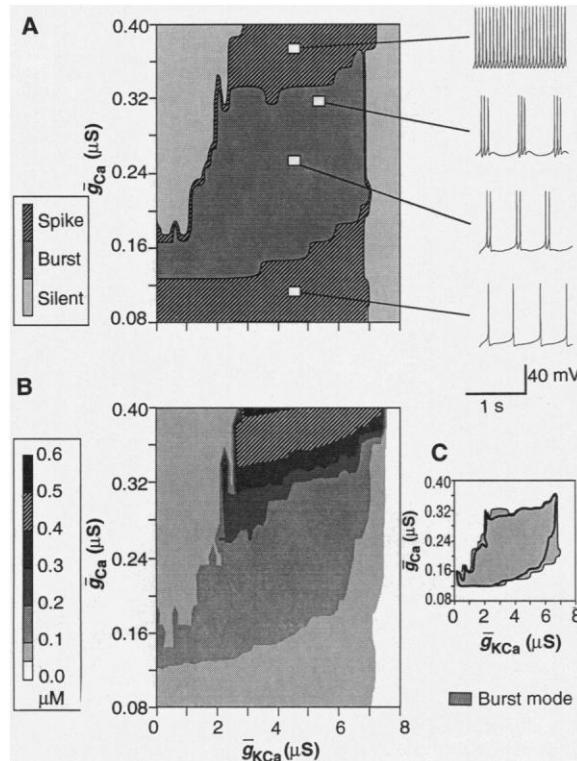
neuron of the stomatogastric ganglion of the crab (*4*). This model has seven active currents—fast Na⁺ ($I_{Na}$), delayed rectifier K⁺ ($I_K$), fast ($I_{Af}$) and slow ($I_{As}$) transient K⁺, hyperpolarization-activated inward ($I_H$), transient Ca²⁺ ($I_{Ca}$), and Ca²⁺-dependent K⁺ ($I_{KCa}$)—as well as a passive leak ($I_L$) current. The maximal conductances of the seven active currents of the model are denoted by $\bar{g}_i$. The model neuron is a single compartment, and Ca²⁺ buffering is described by exponential decay. The results are not specific to this model; we obtained similar results (*5*) using other models (*2, 6*).

The intracellular Ca²⁺ concentration correlates closely with the pattern of electrical activity exhibited by the model neuron (Fig. 1). The maps illustrate activity (Fig. 1A) and time-averaged Ca²⁺ concentration (Fig. 1B) as a function of the maximal conductances of $I_{Ca}$ and $I_{KCa}$. The model neuron shows bursting activity for the central region of this map; in the other regions, it shows high- and low-frequency tonic firing or is silent (either depolarized, "locked up," or hyperpolarized) (Fig. 1A). The time-averaged Ca²⁺ concentration is plotted for the same range of maximal conductances (Fig. 1B). When the neuron is either silent or firing slowly, intracellular Ca²⁺ is low; when the neuron is firing tonically, intracellular Ca²⁺ is high. The superposition (Fig. 1C) shows that bursting activity occurs when the average Ca²⁺ concentration is 0.1 to 0.3 μM. Because the intracellular Ca²⁺ concentration is a reliable indicator of the neuron's electrical

activity, it can serve as an activity-dependent feedback signal for the regulation of maximal conductances.

The dynamic regulation mechanism allows all seven maximal conductances to vary between zero and a maximum value, $G_i$. Modification of a $\bar{g}$ in response to changes of the intracellular Ca²⁺ concentration is a slow process (orders of magnitude slower than, for instance, Ca²⁺ modulation of the Ca²⁺-dependent K⁺ channel). This modification could correspond to Ca²⁺ regulation of channel synthesis, insertion, or degradation. We model the dynamic behavior of the maximal conductances with the equations

$$\tau_i \frac{d\bar{g}_i}{dt} = f_i([Ca]) - \bar{g}_i \tag{1}$$

where $f_i([Ca])$ is a sigmoidal function of the Ca²⁺ concentration, [Ca], and

$$f_i([Ca]) = \frac{G_i}{1 + \exp\{\pm ([Ca] - C_T)/\Delta\}} \tag{2}$$

where $C_T$ is a target Ca²⁺ concentration and $\Delta$ is a parameter that determines the slope of the sigmoid.

The maximal conductance $\bar{g}_i$ relaxes exponentially, with a time constant $\tau_i$, to an asymptotic value determined by $f_i([Ca])$. The Ca²⁺ concentration depends on the electrical activity of the cell, which in turn depends on the values of the maximal conductances, closing the feedback loop. Any factor that modifies the relation between the Ca²⁺ concentration and the maximal conductances shifts the $\bar{g}_i$ values.
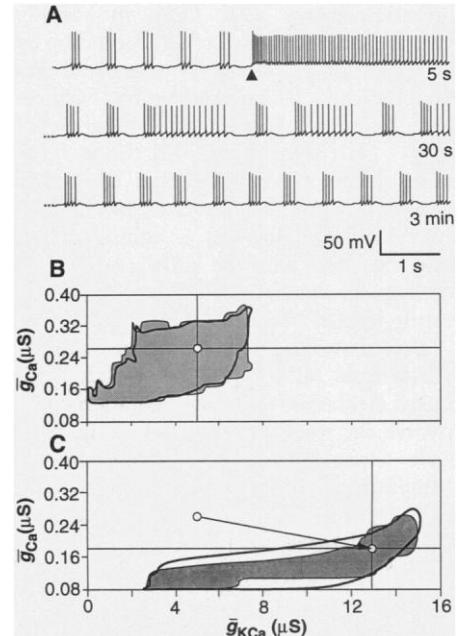
We used a stability criterion to determine the sign in the exponential in Eq. 2. In response to a long depolarization, stability dictates that the resulting Ca²⁺ increase should reduce the inward conductances and increase the outward currents (and vice versa for long hyperpolarizations). Thus, we use a positive sign for inward currents and a negative sign for outward currents.

The values of $\tau_i$ control the approach to equilibrium but do not affect the steady-state behavior. We set all $\tau_i = 50$ s; we expect that a more realistic scale for these time constants would be many minutes or hours, but we accelerated the process to speed up our simulations. Similarly, the values of the $G_i$ are not critical, and we set them to three times the value of the corresponding equilibrium $\bar{g}_i$ under control conditions. The model is sensitive to the values of $C_T$ and, to a lesser extent, $\Delta$. To construct the bursting neuron shown in the figures, we set $C_T = 0.2$ μM and $\Delta = 0.05$ μM. These values assure that for a wide variety of conditions, the dynamic conductance model will ultimately reach a bursting state. A lower value of $C_T$ results in a model that will dynamically maintain silent behavior. If $C_T > 0.2$ μM, the model neuron will fire tonically at a rate that is determined by the value of $C_T$.

This regulation scheme stabilizes the activity of the neuron. If $\bar{g}_i$ values or extracellular ion concentrations are changed and the behavior of the neuron is modified, the maximal conductances will be adjusted and
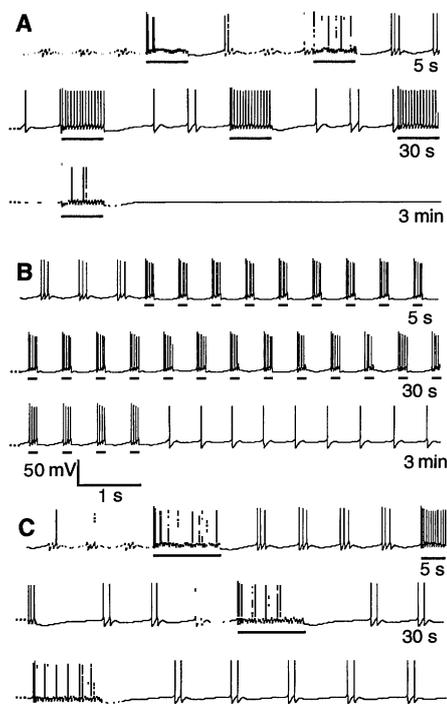
**Fig. 3.** (**A** to **C**) Change in behavior due to different patterns of stimulation. Stimulation with a current of 5 nA is indicated by the bars. Traces show 5-s sweeps ending 5 s, 30 s, and 3 min after the start of the simulation. If the neuron is left unstimulated, in time it returns to its control, prestimulus condition (not shown).



**Fig. 4.** Two identically bursting neurons (1 and 2). In (**A**) they are uncoupled, and in (**B**) they are coupled electrically with a conductance of 0.8 μS. At the time indicated by the arrowheads, $\bar{g}_{Ca}$ is raised in the second neuron and lowered in the first neuron, both by 25%. Traces show 5-s intervals for each cell ending 5 s (top sets of traces) and 3 min (bottom sets of traces) after the start of the simulation.

second-messenger feedback mechanism that regulates maximal conductances can at once stabilize neuronal function and serve as a differentiation mechanism. The concentration of $Ca^{2+}$ correlates with activity (7), and $Ca^{2+}$ is a ubiquitous regulator of biochemical processes that influence neuronal activity (8). Changes in the intracellular $Ca^{2+}$ concentration due to electrical activity can produce protein phosphorylation (9) and induce gene expression (10). Our assumption that ion channel synthesis and degradation could be tied to activity is supported by recent work (11), and experiments inspired by our model that use stimulation of cultured neurons are under way (12).

Most studies of the effects of activity on the formation of neuronal circuits have focused on activity-dependent modifications of synaptic strength (13). However, activity-dependent processes may also modify the intrinsic electrical properties of neurons.

the initial behavior will be restored (Fig. 2). In Fig. 2A at the arrowhead, the equilibrium potential for potassium ($E_K$) was shifted from −80 mV to −65 mV. In response, the neuron started to fire tonically. This activity increased the intracellular $Ca^{2+}$, causing the dynamic regulation process to decrease the inward currents and increase the outward currents until the neuron resumed bursting. The parameter region that produces bursting behavior in normal extracellular $K^+$ shifted when the $K^+$ concentration was increased (Fig. 2C), and the region where the average intracellular $Ca^{2+}$ concentration is 0.1 to 0.3 μM moved with it. The open circle and crossed lines in Fig. 2B show the values of $\bar{g}_{Ca}$ and $\bar{g}_{KCa}$ that produced bursting behavior (Fig. 2A) initially. The initial maximal conductances are also shown as the open circle in Fig. 2C. After $E_K$ was shifted, the maximal conductances moved to the final point indicated by the open circle and crossed lines in Fig. 2C and bursting resumed.

The same mechanism that stabilizes an isolated neuron also maintains its electrical activity pattern in a network. A model neuron in a network may have different maximal conductances than when it is in isolation, and injected current pulses can shift its maximal conductances. Figure 3, A

to C, shows the response of a model neuron to the same total stimulation (bars) but delivered in three different patterns. After a brief control period, during which the initial bursting activity of the neuron is seen, stimulation begins. After 3 min, the stimulation is stopped, revealing that the intrinsic behavior of the neuron has changed. In Fig. 3A the neuron became silent, in Fig. 3B it became tonically active, and in Fig. 3C it became a weak burster.

Dynamic regulation may play a role in network development. Two uncoupled neurons appear in Fig. 4A. At the arrowhead, $\bar{g}_{Ca}$ was raised in one cell and lowered in the other. In response, the dynamic mechanism restored both to their original pattern of activity (Fig. 4A). When the two neurons were electrically coupled (Fig. 4B), the same perturbations of the individual neurons resulted in a bursting circuit, with the two neurons firing somewhat differently (initial part of lower two traces in Fig. 4B). When we removed the coupling between the two neurons to examine their individual properties, they exhibited different intrinsic characteristics, although the two symmetrically coupled neurons were described by identical sets of equations (5).

The model described here shows that a

**REFERENCES AND NOTES**

1. I. R. Epstein and E. Marder, *Biol. Cybern.* **63**, 25 (1990).
2. R. E. Plant and M. Kim, *Biophys. J.* **16**, 227 (1976); J. Rinzel and Y. S. Lee, *J. Math. Biol.* **25**, 653 (1987).
3. F. Buchholtz, J. Golowasch, I. R. Epstein, E. Marder, *J. Neurophysiol.* **67**, 332 (1992); J. Golowasch, F. Buchholtz, I. R. Epstein, E. Marder, *ibid.*, p. 341.
4. J. Golowasch and E. Marder, *ibid.*, p. 318.
5. L. F. Abbott and G. LeMasson (*Neural Comput.*, in press) discuss these models and present a mathematical analysis of dynamic regulation of maximal conductances.
6. C. Morris and H. Lecar, *Biophys. J.* **35**, 193 (1981).
7. W. M. Ross, *Annu. Rev. Physiol.* **51**, 491 (1989).
8. M. B. Kennedy, Ed., *Trends Neurosci.* (special issue) **12**, 417–479 (1989); H. Rasmussen and P. Q. Barrett, *Physiol. Rev.* **64**, 938 (1984).
9. L. K. Kaczmarek, *Trends Neurosci.* **10**, 30 (1987); J. E. Chad and R. Eckert, *J. Physiol. (London)* **378**, 31 (1986); L. K. Kaczmarek and I. B. Levitan, Eds., *Neuromodulation: The Biochemical Control of Neuronal Excitability* (Oxford Univ. Press, New York, 1987).
10. M. Sheng and M. E. Greenberg, *Neuron* **4**, 477 (1990); J. I. Morgan and T. Curran, *Annu. Rev. Neurosci.* **14**, 421 (1991); T. H. Murphy, P. F. Worley, J. M. Baraban, *Neuron* **7**, 625 (1991); L. M. Hemmick *et al.*, *J. Neurosci.* **12**, 2007 (1992).
11. J. L. Franklin, D. J. Fickbohm, A. L. Willard, *J. Neurosci.* **12**, 1726 (1992).
12. G. G. Turrigiano, G. LeMasson, L. F. Abbott, E. Marder, unpublished results.
13. J. H. Byrne and W. O. Berry, *Neural Models of Plasticity* (Academic Press, San Diego, 1989); M. A. Gluck and D. E. Rumelhart, *Neuroscience and Connectionist Theory* (Erlbaum, Hillsdale, NJ, 1990); M. Constantine-Paton, H. T. Cline, E. Debski, *Annu. Rev. Neurosci.* **13**, 129 (1990).
14. All figures were generated on a Macintosh IIfx computer with MAXIM, a software system for simulating single neurons and neural networks, developed by G. LeMasson. In Figs. 1 and 2 we use $I_{Ca}$ and $I_{KCa}$ as typical examples; other pairs give similar results.
15. Supported by National Institute of Mental Health grant MH46742, National Science Foundation grant DMS-9208206, and the Human Frontier Science Program Organization. We thank J. McCarthy for manuscript preparation.

19 August 1992; accepted 29 December 1992